Chalcogenide Letters Vol. 8, No. 2, February 2011, p. 65 – 75

A COMPARATIVE STUDY OF BSF LAYERS FOR ULTRA-THIN CdS:O/CdTe SOLAR CELLS

M. A. ISLAM[a*], YUSUF SULAIMAN[b], NOWSHAD AMIN[a,b]
[a]*Department of Electrical, Electronic and System Engineering National University of Malaysia, Bangi, 43600 Selangor, Malaysia*
[b]*Solar Energy Research Institute, Universiti Kebangsaan Malaysia, Malaysia Nasional, Kajang 43009, Selangor, Malaysia*

Due to high electron affinity and consequently large work function of CdTe, the CdTe based solar cells are suffering from ohmic contacting problem at the back contact. Among the several numbers of methods still used try to overcome the ohmic contacting problem, the use of back surface field (BSF) material is found to be better, effective and easier one. The conventional CdS/CdTe solar cell was modified by nano-crystalline CdS:O window layer and Sb_2Te_3, As_2Te_3 and ZnTe as a BSF layer inserted after the CdTe layer. The cell performances are investigated by detailed described on external quantum efficiency (QE), and dark and light I-V characteristics by recognized simulator 'Analysis of Micro-electronics and Photonic Structures' (AMPS-1D). The temperature and light intensity variation effects also described to understand the environmental effect on the cell performance. The results have shown that the BSF layers enhance the cell performances and have no adverse effect on cell stability as the condition of circumstance are changed. However, the results have shown that the structure ZnO/CdS:O/CdTe/Sb_2Te_3/Ag gives highest efficiency, exhibits a low series resistance and high shunt resistance also. The cell with ZnTe is shown to produce important series resistance problems because of an unfavorable hetero-junction with CdTe.

(Received January 28, 2011; accepted February 2, 2011)

Keywords: CdTe thin film solar cell, CdS:O window layer, BSF layers, AMPS-1D.

1. Introduction

At present, the CdTe solar cell makes more attraction to the researchers and commercials for its higher efficiency, low cost, highly stable and large scale fabrication opportunity. CdTe has larger absorption co-efficient (>5×10^5/cm) due to its ideal and direct band gap energy 1.45 eV; which corresponds well to sunlight spectra and ~99% of photons with energy greater than the band gap (E_g) can be absorbed within 1 μm of CdTe film [1, 2, 3]. Small-area CdTe cells already achieved efficiency of 16.5% in laboratory and 11% in commercial modules. The polycrystalline CdS has found to be the best-suited hetero-junction n-type partner with p-type CdTe absorber for CdS/CdTe solar cell. But CdS has the three main issues that limit the CdTe Cell performance which has been reported and a novel window material nano-crystalline CdS:O film has been proposed [4, 5]. However, the energy gap of CdS window layer is 2.42 eV, so it absorbed the light at wavelengths below 510 nm and make energy loss in the cell about 20% [6]. The advantages of CdS:O window layer over CdS have been reported [7].

*Corresponding author: aminbgm@yahoo.com

Another major challenge associated with the fabrication of efficient CdTe based solar cells are formation of stable and low resistive back contact to p-CdTe. It is difficult due to large electron affinity and low native carrier concentration of CdTe [8]. An ohmic contact to CdTe requires either a metal with a work function greater than 5.7 eV or a sufficiently narrow Schottky barrier to enable tunneling. No metal have been found which have such large work function (>5.7eV) to match properly with CdTe and so, there're naturally exist a wide Schottky barrier between the CdTe and Metal back contact. Various techniques used for the contact formation have been extensively reviewed [9]. To overcome such a problem, generally a Cu containing back contact is generally used which creates a quasi ohmic, non-rectifying contact and additionally dopes the CdTe layer. These types of cells exhibit good efficiencies in the beginning; however the efficiency degrades with time due to Cu diffusion to the front contact which causes shunting effect [10]. Another strategy to overcome the naturally existing Schottky barrier is to create a heavily p-doped CdTe surface by chemical etching and apply a buffer layer or back surface field (BSF) materials of high carrier concentration and low resistive between CdTe and the metal [11, 12]. This process decreases the barrier width at the back contact interface. The tunneling barrier formed in this way is quasi ohmic and also acts as a minority carrier mirror.

An efficient back surface field is an indispensable structural element to attain high efficiency in a solar cell. The importance of BSF layers in the field solar cells attracted some attention in the 1980s [13, 14, 15]. The main role of this layer is to provide confinement for the photo-generated minority carriers and keep them within the reach of the p-n junction to be efficiently collected. This has to be accomplished without increasing the series resistance of the device. Additionally, photon confinement capabilities are an interesting ancillary property for good BSF layer.

The goal of this paper is to find out a higher efficiency and more stable CdTe solar cell by introducing BSF layer. We investigate a better BSF layer that would be well suited to CdTe and back contact metal. We consider three types of semiconductor materials such as As_2Te_3, Sb_2Te_3 and ZnTe and investigated their performance as a BSF layer by AMPS-1D simulator. To understand extensively the effect of BSF layers on cell's general performance parameters and shunt and series resistance more emphasize given to the external quantum efficiency (QE), dark and light I-V and hetero-junction band diagram between CdTe and BSF layers. The temperature and light intensity also taken under consideration to understand the environmental effect on the cell performance.

2. Modeling and simulation

The major objectives of numerical modeling and simulation in solar cell research are testing the validity of proposed physical structures, geometry on cell performance and fitting of modeling output to experimental results. Any numerical program capable of solving the basic semiconductor equations could be used for modeling thin film solar cells. The fundamental equations for such numerical programs are (i) Poisson's equation for the distributions of electric field (φ) inside the device and (ii) the equation of continuity for conservation of electrons and holes currents. An ideal thin film solar cell simulator is developed by considering the minimum condition as mentioned in the table. I [16]

Table I. Critical issue for a thin film PV simulation program.

No. of issues	Descriptions
1	Multiple layers (minimum should be six layers) able to be adopt.
2	Should be maintain large Band gaps; usually; $E_g \geq$ 1-3.7 eV.
3	Band discontinuities in E_c and E_v; i.e., ΔE_c and ΔE_v should be taken under consideration.
4	Recombination and charge in deep bulk states should be able to explain.
5	Simulation and charge in deep interface states should be able to explain.
6	Graded band gaps; E_g (x) also χ(x), N_c(x), α(x) etc should be taken under consideration.
7	Non routine simulation could be measured.
8	J-V, C-V, C-f, QE(λ) ,.....all will be explained as a function of T.
9	It should be fast and easy to use.

The AMPS-1D program has been developed for pragmatically simulate the electrical characteristics of thin film hetero-junction solar cells. It has been proven to be a very powerful tool in understanding device operation and physics for single crystal, poly-crystal and amorphous structures. To date, more than 200 groups worldwide have been using AMPS-1D for solar cell design [17]. One-dimensional AMPS-1D simulator has been used to investigate the effect of different BSF layers. Fig. 1a and 1b shows the structure of conventional CdS/CdTe solar cell and modified with CdS:O window layer and different BSF layers. First, a three layers CdS/CdTe solar cell as shown in fig. 1(a) considered as a base cell, then we changed CdS window layers by CdS:O and insert different BSF layers before the back contact Ag. The CdS:O layers thickness was varied from 10 nm to 100 nm and the change of performance parameters are observed. The BSF layers thickness also changed from 100 nm to 500 nm with fixed 50 nm CdS:O cell. The operating temperature and light intensity have been changed from 25 ^{0}C to 150 ^{0}C and 0.01 suns to 1000 suns, respectively. The base parameters used for different structures adopted from some standard references [18, 19, 20] are shown in Table II.

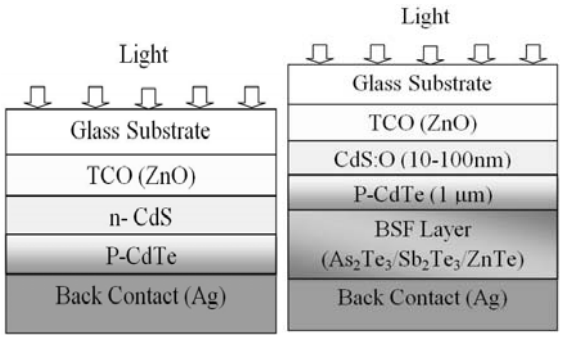

Fig. 1(a). Conventional CdS/CdTe solar cell and 1(b). modified CdS:O/CdTe solar cell.

Table II. Parameters used In simulation.

Parameters	ZnO	n-CdS:O	p-CdTe	Sb_2Te_3/As_2Te_3 /ZnTe
Thickness, W (μm)	0.5	0.01-0.10	1.00	0.10-0.50
Relative permittivity, $\varepsilon/\varepsilon_0$	9.0	10.0	9.4	55/20/14
Electron mobility, μ_c (cm^2/Vs)	100	100	320	1094/500/70
Hole mobility, μ_p (cm^2/Vs)	25	25	40	320/2100/50

Acceptor/donor concentration, n, p (cm^{-3})	1.0×10^{18}	1.0×10^{16}	5.0×10^{15}	$(6.8/6.8/0.1)\times 10^{19}$
Band gap, E_g (eV)	3.3	2.75	1.50	0.42/0.6/2.25
Effective density of states in conduction band, N_c (cm^{-3})	2.2×10^{18}	1.8×10^{19}	7.5×10^{17}	$(1.0/1.0/70)\times 10^{16}$
Effective density of states in valance band, N_v (cm^{-3})	1.8×10^{19}	2.2×10^{18}	1.8×10^{18}	$(1.0/1.0/200)\times 10^{17}$
Electron affinity, χ (eV)	4.50	4.50	4.28	4.15/4.0/3.65

3. Results and discussion

The simulation work has been performed aiming to compare the different types of cell structure made by changing BSF materials to find out best structure for higher efficiency and more stable CdS:O/CdTe solar cells. We consider three types of cell structures by insertion semiconductor materials such as As_2Te_3, Sb_2Te_3 and ZnTe and investigated their performances as a BSF layer by AMPS-1D simulator. The effect of BSF layers on cell performance such as effect on general performance parameters, quantum efficiency (QE), shunt and series resistance, light and dark I-V characteristics and hetero-junction band diagram between CdTe and BSF layers are described. The highest outputs for 50 nm CdS:O layers with 100 nm BSF and without BSF layers are shown in Table-III.

Table III. Associated performance for solar cell with different BSF layers.

Structure	Voc (V)	Jsc (mA/cm^2)	FF	η (%)
As_2Te_3 BSF, ZnO/CdS:O/CdTe/As_2Te_3/ Ag	0.976	28.96	0.83	21.35
Sb_2Te_3 BSF, SnO2/CdS:O/CdTe/Sb_2Te_3/Ag	0.976	28.93	0.84	21.37
ZnTe BSF, ZnO/CdS:O/CdTe/ ZnTe/Ag	0.973	28.92	0.76	19.51
Without BSF, ZnO/CdS:O/CdTe/Ag	0.948	27.36	0.78	18.44

3.1 CdS:O Layer Thickness Effect

The three layer device with 1 μm CdTe absorber layer was modified by CdS:O window layer and Sb_2Te_3 / As_2Te_3 / ZnTe BSF layer. The effects of CdS:O layer thickness variation from 10 nm to 100 nm on the cell output parameters were observed to acquire the optimum window layer thickness and the effect on short circuit current (*Jsc*) and efficiency (*η*) have shown in the fig. 2. Here, the *Jsc* is increased with reduction of CdS:O layer thickness as expected.

However, the conversion efficiency is increased with reduction of CdS:O layer thickness until 50 nm but below 50 nm it shows a decreasing trend; behinds on it that the *Voc* and FF are increased as the increase of thickness till 50 nm but after 50 nm, almost no change. So, 50 nm CdS:O layer thickness is enough for optimum conversion efficiency. At very thin CdS:O layer, may be dominate pin hole effect and shunt effect at the p-n junction for which the efficiency as well as *Voc* and FF of the cell goes down.

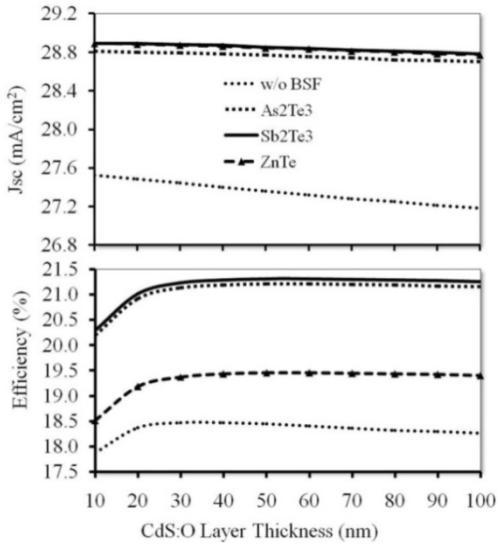

Fig. 2. The effect of CdS:O layer on cell efficiency and Jsc

The 50 nm CdS:O layer with 500 nm BSF layer shows the highest conversion efficiency of 20.91% as shown in fig. 2. The improvement in efficiency cames from insertion of higher band gap CdS:O layer, which eliminate the unwanted diffused $CdTe_{1-x}S_x$ layer of lower band gap(~ 1.4 eV), improved QE and reduced window layer thickness respectively [4]. This work has been published in 2010 [21]. Moreover in fig. 2, we have seen that the efficiency goes rise due to insertion of BSF materials at the back contact. BSF layer make a bridge between the CdTe absorber layer and the back contact, minimize the junction mismatch and reduced the back contact Schottkey barrier height respectively. Moreover, BSF layer decrease the loss of carriers at the back contact by reducing the carriers recombination and reflecting the carriers towards the P-N junctions, and increase the cell efficiency [20].

3.2 External Quantum Efficiency

The spectral response (QE) for different BSF materials from AMPS-1D simulation is shown in fig. 4. The graph has shown that the BSF layers pick up the cell external quantum efficiency. The cell with BSF layers As_2Te_3 and

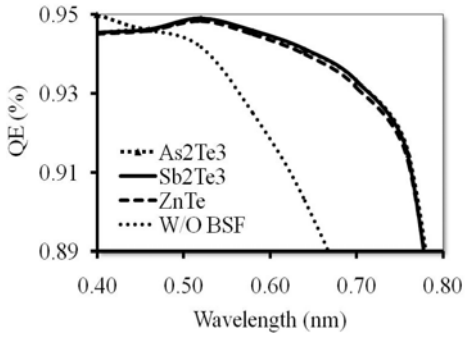

Fig. 4. The QE curve of the cells with different and without BSF layers.

Sb_2Te_3 have an indistinguishable performance. However, the cell with BSF layers maintains almost above 91% of QE for the whole visible range of spectra where it is confirmed better energy conversion performance of the cell.

3.3 Dark I-V characteristics

The dark I-V curves also have drawn to gain more insight into the internal performance such as the series and shunt resistance of the cells. It is well known that the dark current-voltage relationship of solar cell device can be written as follow [22].

$$I = \frac{V - IR_S}{R_{Sh}} + I_{OR}\left[exp\left\{\frac{q(V - IR_S)}{2kT}\right\} - 1\right] + I_{OD}\left[exp\left\{\frac{q(V - IR_S)}{2kT}\right\} - 1\right] \quad (1)$$

where, the I_{OR} and I_{OD} stand for recombination and diffusion saturation currents. All the other symbols have their usual meanings. In order to obtain values for all parameters involved in equation (1), we need to make some approximations, depending on the value of the voltage. From the two diode model it can be interpreted that at high voltages, the series resistance dominates in the dark I-V characteristics, at the mid range of the voltage; the generation and recombination compounds are predominant and at the low voltage region, the shunt resistance is predominates [18, 23]. By solving the equation (1) following the procedure described in [24, 25] we can find out, the series resistance at high voltage values,

$$Y = -\frac{kT}{qR_S} + \frac{1}{R_S}X \quad (2)$$

the total current in generation and recombination,

$$I \approx I_{OR}\left[exp\left(\frac{qV}{kT}\right) - 1\right] + \frac{V}{R_{Sh}} \quad (3)$$

and the shunt resistance at the low voltage

$$I \approx \frac{V - IR_S}{R_{Sh}} \quad (4)$$

The dark I-V curve have found in the simulation have shown in the fig. 5. The influence of series and shunt resistances are clearly seen in the fig. 5. Following the equations (2) and (4), we have determined the R_S value for voltages higher than 1.1 V and R_{sh} value for voltage lower than 0.5 V for the cell of different BSF layers. These are shown in the table III.

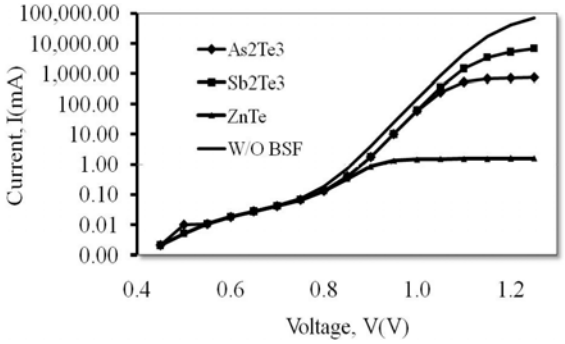

Fig. 5. Dark I-V characteristics of different cell.

Table IV. The Series and Shunt Resistance exhibit by Different Cell at Room Temperature

Cell with	As_2Te_3	Sb_2Te_3	ZnTe	W/O BSF
R_s at 1.1 Volt	2.0 Ω	0.71 Ω	688 Ω	0.24 Ω
R_{sh} at 0.5 Volt	4998 Ω	499.2 Ω	4312 Ω	499.76 Ω

It is clear from the fig. 5 and table IV that, every cell maintains a high shunt resistance at the low voltage region. But at high voltage region, the cell with BSF layer exhibits a resistive loss more than cell without BSF layers. So, the BSF layer introduces a little bit series resistance but this effect goes behind due to other positive effect that enhances the efficiency of the cell. The cell with As_2Te_3 and Sb_2Te_3 BSF layers shown the series resistance in a considerable region but the cell with ZnTe BSF layer is shown an unexpected large series resistance. Why ZnTe exhibits more series resistance than others and why it is so large? This phenomena was tried to understand from band diagram which shown in fig. 6. Here, the fig. 6 has shown that for minority carrier's reflection, all the BSF layers at the conduction bands are very good. However it is also evident that there exists an important barrier in the valance band at the CdTe/ZnTe hetero-junction (almost 0.06 eV) which cause for unexpected behaviors of ZnTe under dark and increase cell series resistance. Due to the large valence band offset as shown in fig. 6, As_2Te_3 exhibit more resistance than Sb_2Te_3 but As_2Te_3 has also a large conduction band offset which act as an excellent minority carrier reflection.

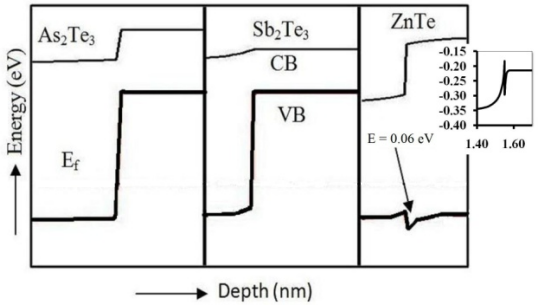

Fig. 6. Band diagram of As_2Te_3, Sb_2Te_3 and ZnTe hetero-junction with CdTe absorber layer

3.3 Light I-V characteristics

The light J-V characteristic of the different cells with 100 nm BSF layers found by AMPS-1D simulation is shown in fig. 7. The simulated J-V curve shows that the output characteristics of the cell with BSF layers are confirming higher *Jsc, Voc* and FF than the cell without BSF layer. The structure with BSF showed higher *Voc, Jsc* and FF than the cell without BSF due to reduced back surface recombination and improved back contact formation with p-CdTe. Thus, the conversion efficiency of the cell with BSF is higher than without BSF layer.

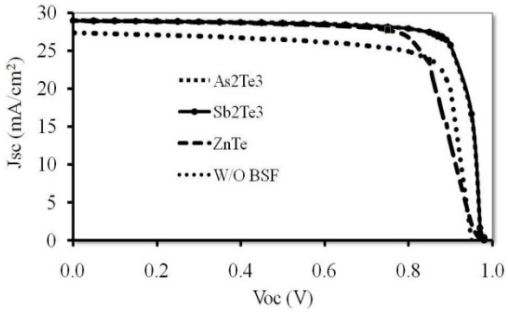

Fig. 7. The light J-V characteristics curve for without and with different BSF layers.

3.5 Temperature effects

It is well known that the operating temperature plays a very important role for every kind of solar cell performances. At higher operating temperature, parameters such as the electron and hole mobility, carrier concentrations, density of states and band gaps of the materials are affected [26]. In order to investigate the effects of higher operating temperature on cells performances; simulation were carried out with cell operating temperature ranged from 25°C to 150°C and the simulated results are shown in fig. 8. The effect of temperature measured by the term named temperature coefficient, which means the change of power of solar cell for increase or decrease of operating temperature per degree centigrade.

The normalized temperature coefficient (1/η dη/dT) can be resolved into the sum of the Variations of the open circuit voltage (*Voc*), the short circuit current (*Jsc)*, and the fill factor (FF) [27]:

$$\frac{1}{\eta}\left(\frac{d\eta}{dT}\right) = \frac{1}{Voc}\left(\frac{dVoc}{dT}\right) + \frac{1}{Jsc}\left(\frac{dJsc}{dT}\right) + \frac{1}{FF}\left(\frac{dFF}{dT}\right) \qquad (5)$$

By simplifying and calculating the semiconductor equations we find that the operating temperature dependence of short-circuit current, 1/Jsc dJsc/dT<<10^{-3} per ^{0}C and the operating temperature dependency FF, 1/FF dFF/dT<< -10^{-3} per ^{0}C. Therefore, the operating temperature effect on *Jsc* and FF of solar cell is too little. Furthermore, the voltage change equation against operating temperature is [28]

$$\frac{dVoc}{dT} = -\frac{\left\{Vgo - Voc + \gamma\left(\frac{kT}{q}\right)\right\}}{T} \qquad (6)$$

Where:
V_{go} is the band gap linearly extrapolated to absolute zero; T is the operating temperature; k is the Boltzmann constant; q is the electronic charge and γ is an arbitrary constant to incorporate the possible operating temperature dependencies of the other material parameters.

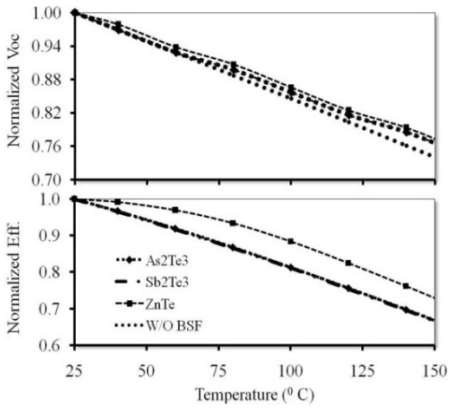

Fig. 8. The temperature effect on cell efficiency and Voc.

The above two equations show that the operating temperature sensitivity of a solar cell depends on its open circuit voltage and the cell with higher open circuit voltage is less affected by temperature. As the cell operating temperature rise up, the band gap decreases, and hence the cell responds to longer wavelength portions of the spectrum, and therefore the short circuit current actually increases but little with operating temperature [29]. Moreover, it also theoretically and practically proved that *Voc* also decrease with decrease of band gap (Vgo) and since the *Voc* variation contributes most the change in efficiency as mentioned above; so, with increase of operating temperature ultimately decrease the efficiency of the cell.

The fig. 8 has shown that the cells with As_2Te_3, Sb_2Te_3 and without BSF follow the same trends with increase of temperature and their temperature coefficients are 0.25%. But it is surprised to observe that the cell with ZnTe BSF layer has shown a better stability against temperature than others by the temperature coefficient 0.1%. Furthermore, the cell without BSF layer rapidly goes to decrease Voc than cell with BSF layers under the temperature increase. Thus, the BSF has some constructive effects on the cell stability at higher operating temperature.

3.6 Effect of Light Intensity

We know that the light intensity is changed with respect to the terrestrial places. Moreover, solar cells experience daily variations in light intensity, with the incident power from the sun varying from '0' to '1' kW/m^2, so it is important to investigate the effect on solar cell parameter with the variation of light intensity.

The variation in the incident light intensity on a solar cell changes all solar cell parameters, including the short-circuit current, the open-circuit voltage, the FF, the efficiency and the impact of series and shunt resistances. The light intensity on a solar cell is called the number of suns, where 1 sun corresponds with standard illumination at AM1.5, or 1 kW/m^2.

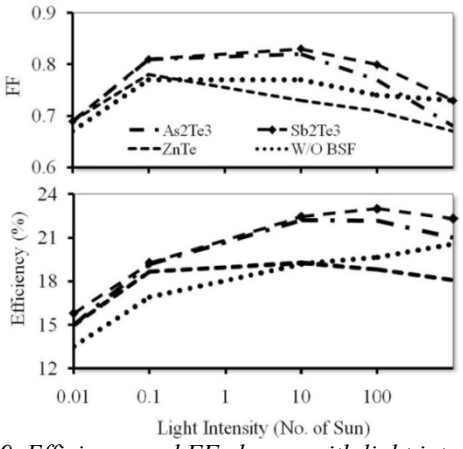

Fig.9. Efficiency and FF change with light intensity

The short-circuit current from a solar cell depends linearly on light intensity, but *Voc* increases logarithmically with light intensity. Fig. 9 shows the change of efficiency and FF with logarithmic change of sun intensity. The efficiency increase for increase of light intensity till 100 sun for As_2Te_3 and Sb_2Te_3 but till 10 suns for ZnTe cell, after that all the cell show a decreasing trend. This may have happened due to the increase in electron-hole recombination, temperature of front contact and series resistance respectively at higher light intensity [30].

To understand the relation of series resistance with the variation of light intensity, the FF vs sun intensity curve isshown in fig. 9. It is well known that FF is directly affected by series resistance of a solar cell. If the series resistance increases, the FF goes decreases. Moreover, the fig. 9 has shown that the FF decreases more in ZnTe cell than others, i.e. the series resistance of the cell with ZnTe BSF layer increase rapidly under the increase of light intensity. On the other hand, the cell with As_2Te_3 and Sb_2Te_3 preserve a constant series resistance until 10 suns, after that As_2Te_3 shows more series resistance than Sb_2Te_3.

4. Conclusions

Three different structures with CdS:O window layer have been analyzed by AMPS-1D simulator. Due to high band gap and reduce the inter-diffusion tendency at the p-n junction; CdS:O window layer improve cell performance over the CdS. The uses of BSF layer improves the cell performance by produce mirror for minority carriers and by reduce the Schottky barrier height. The main results obtained for the each BSF layer associated with cell performances are as follows:

BSF layer As_2Te_3 shows high shunt resistance and moderate series resistance. It exhibits a little bit more series resistance due to high valence band offset with CdTe absorber layer. As the light intensity increases, the series resistance of the cell increases. It also acts as an excellent minority carrier reflector due to its high conduction band offset so it can overcome the problem introduces by series resistance and exhibit high solar cell performance. BSF layer Sb_2Te_3 exhibit the outstanding performance in over all conditions. The main reasons for these are; a low valence band offset to CdTe, which produces low series resistance for majority carriers, and high conduction band offset to CdTe, which produce an excellent mirror for minority carriers. BSF layer ZnTe exhibit almost poor performance. Although its minority carrier reflection is high but it has a spike on the valence band which produces high series resistance for majority carriers of the cell. This large series resistance affects the all parameters of the cell as evidenced by external quantum efficiency measurements, dark and light I-V curves, band diagram and light intensity variation measurements.

Acknowledgements

This work is supported by the department of Electrical, Electronics & System Engineering and Solar Energy Research Institute (SERI) of the National University of Malaysia through the research grant UKM-GUP-TK-08-16-058.

References

[1] J. Britt, C. Ferekides, Applied Physics Lett. **62**(22), 2851(1993).
[2] Xuanzhi Wu, Solar Energy (77), 803 (2004).
[3] M. Hadrich, C. Kraft, C Loffler, H. Metzner, U. Reislohner, W. Witthuhn, Thin Solid Films, **517**, 2282 (2009).
[4] X Wu et al., Proceedings of 29th IEEE PVSC, May 19-24, 2002, New Orland, Louisiana.
[5] McCandess, B.E., Hegedus, S.S., Proceedings of 22nd IEEE PVSC, Oct. 7-9, 1991, Las Vegas, NV, USA.
[6] Toshiro Maruyama, Ryota Kitamura, Transformations of the Wavelength of the Light Incident Upon CdS/CdTe Solar Cells, Solar Energy Materials and Solar Cells, **69**, 2001,

pp. 61-68.
[7] Aminul Islam, M. A. Matin, Yusuf Sulaiman and Nowshad Amin, 1st International Conference on the Developments in Renewable Energy Technology (ICDRET), December 17-19, 2009, Dhaka, Bangladesh.
[8] Joel N. Duenow, Ramesh G. Dhere, Jian V. Li, Matthew R. Young, and Timothy A. Gessert, 35th IEEE Photovoltaic Specialist Conference, 2010, Hawaii.
[9] Lee, Y.J. Gray, J.L., The 22ND IEEE Photovoltaic Specialist Conference, pp. 1151-1155, Oct 9-11, 1991, Las Vegas, NV.
[10] D.L. Batzner, A. Romeo, H. Zogg, A.N.Tiwari and R. Wendt, E-MRS Conference, 2000, Strasbourg.
[11] J. Sarlund, M. Ritala, M. Leskela, E. Siponmaa, R. Zilliacus, Solar Energy Materials and Solar cells **44**, 177 (1996).
[12] C.S. Ferekides, V. Viswanathan, D.L. Morel, Proceedings of the 26th Photovoltaic Solar Energy Conference, 1997, Aneheim.
[13] Gale R P, Fan J C C, Turner G W and Chapman R L, Proc. 17th IEEE Photovoltaic Specialists Conference, 1984, NewYork, USA.
[14] DeMoulin P D, Lundstrom M S and Schwartz R J, Solar Cells: Sci., Technol., Appl. Econ, **20**, 229 (1987).
[15] DeMoulin P D and Lundstrom M S, IEEE Trans. Electron Devices 36, 897 (1989).
[16] M. Burgelman, John Verschraegen, Stefaan Degrave and Peter Nollet, Prog. in Photovolt: Res. and Appl. **12**,143 (2004).
[17] Hong Zhu, Ali Kaan Kalkan, Jingya Hou and Stephen J. Fonash, AIP Conf. Proc., March 5, 1999. Osaka, Japan.
[18] M. Gloeckler, A.L. Fahrenbruch, and J.R.Sites, 3rd World Conference on Photovoltaic Energy Conversion, May 11-18, 2003 Osaka, Japan.
[19] Arturo Morales-Acevedo, Solar Energy, 80, 675 (2006).
[20] Nowshad Amin, Kamaruzzaman Sopian, Makoto Konagai, Solar Energy Materials & Solar Cells, **91**, 1202 (2007).
[21] M. Wolf, G.T. Neol and R. J. Strin, IEEE Trans. Electron Dev., **24**, 419 (1977).
[22] J. Selinger, Acta Polytechnica, 4, 2006.
[23] D. Fuchs and H. Sigmund, Solid State Electron, **29**, 791 (1986).
[24] I. Martil and G. Gonzalez Diaz, Eur. J. Phys., 13, 193 (1992).
[25] Beatriz Galiana, Ignacio Rey-Stolle, Mathieu Baudrit, Iván García and Carlos Algora, Semicond. Sci. Technol. **21**(10) , 1387 (2006).
[26] J. Fan, Solar Cells **17**, 309 (1986).
[27] G. Landis, Proc. XIII Space Photovoltaic Research and Technology Conference, NASA CP-3278, June 1994, NASA, Lewis Research Center, USA.
[28] Martin A. Green, Solar Cells Operating Principle, Technology and System Applications, Prentice-Hall, New Jersey (1982)
[29] Vinod Vikram L. Dalal and Arnold R. Moore, J. Appl. Phys. **48**, 1244 (1977).